RSC Advances

PAPER

View Article Online
View Journal | View Issue

Cite this: *RSC Adv.*, 2023, **13**, 7561

PSS-dispersed dopamine triggered formation of PAA adhesive hydrogel as flexible wearable sensors†

Xinyu He,[ab] Nuan Wen,[ab] Wei Zhang,[ab] Shuai He,[ab] Shuang Yang,[ab] Xinhua Li,[ab] Chaoxi Chen*[c] and Fang Zuo *[ab]

Catechol-based hydrogels have good adhesion properties; however, since the concentration of catechol is low and it can be easily oxidized to quinone, the adhesion performance of the hydrogels is reduced, which limits their application as self-adhesive flexible wearable sensors. In this work, a dopamine: poly(sodium 4-styrenesulfonate) (DA:PSS)-initiated strategy was proposed to construct adhesive hydrogels, where the semiquinone radicals present in DA:PSS were used to initiate radical polymerization to obtain the DA:PSS/poly(acrylic acid) (DA:PSS/PAA) hydrogel. This hydrogel exhibited good stretchability and adhesion with various substrates. We observed that, even after exposure to air for 21 days under certain relative humidity (76%), the catechol groups hardly oxidized and the DA:PSS/PAA hydrogel presented good adhesion. The DA:PSS/PAA hydrogel also showed good electrical conductivity and fast response ability. Thus, the general strategy of triggering monomer polymerization to form hydrogels based on the semiquinone radical present in DA:PSS offers great potential for their application in flexible electronic devices and wearable sensors.

Received 15th November 2022
Accepted 27th February 2023

DOI: 10.1039/d2ra07243b

rsc.li/rsc-advances

1. Introduction

Adhesive hydrogels, owing to their excellent electronic properties and the soft nature of the wet tissues in them, are great candidates for use in flexible wearable sensors, human movement detection, soft robotics, and wearable healthcare tracking.[1–3] Recently, inspired by natural mussel adhesion, various catechol-based adhesive hydrogels have been proposed in the synthesis of self-adhesive epidermal sensors.[4–6]

So far, several catechol-based adhesive hydrogels have been fabricated using catechol-containing polymers, catechol-functionalized monomers, and other catechol-functionalized materials.[4–14] Dopamine (DA), an important neurotransmitter found in the brain, contains both catechol and amine groups.[15] It is also identified as a small-molecule mimic of mussel foot proteins, which can undergo autooxidation and then self-polymerize under alkaline conditions to generate polydopamine (PDA) materials.[15–22] DA derivatives and PDA-incorporated hydrogels exhibit strong adhesiveness toward various organic and inorganic substrate surfaces, and human skin.[8–12] Radical polymerization using additional initiators is a typical method to prepare mussel-inspired hydrogels.[8–12] However, since the presence of a high concentration of catechol moieties can result in the substantial quenching of free radicals thereby suppressing the formation of hydrogel networks, it is important to ensure that the hydrogels prepared by radical polymerization possess low catechol content, that is, lower than 2 wt% of the monomer.[8–12] However, such a low concentration of catechol undermines the adhesion performance of mussel-inspired hydrogels as well as their application in self-adhesive skin-like sensors. In addition, the catechol in the adhesive hydrogels was usually oxidized to quinone by air during storage and usage, which caused the hydrogels to lose their adhesion ability.[13,14]

Furthermore, Zhang and co-workers found that semiquinone radical species generated during the oxidation of DA can trigger the polymerization of acrylate monomers to eliminate the use of additional free-radical initiators.[23] The Zhang group present a DA-triggered gelation to fabricate mussel-inspired conductive hydrogels with high optical transparency and catechol content (up to 50 wt% of the monomer), simultaneously, by taking advantage of intriguing mussel-inspired chemistry to eliminate the use of additional free-radical initiators.[12]

Recently, the Liang group found that the sulfonate in poly(-sodium 4-styrenesulfonate) (PSS) interacts with the amino group on DA, which inhibits both its cyclization and

[a]College of Chemistry & Environment, Southwest Minzu University, Chengdu 610041, China. E-mail: polymerzf@swun.cn

[b]Key Laboratory of Pollution Control Chemistry and Environmental Functional Materials for Qinghai-Tibet Plateau of the National Ethnic Affairs Commission, Southwest Minzu University, Chengdu 610041, China

[c]College of Animal Science & Veterinary Medicine, Southwest Minzu University, Chengdu 610041, China. E-mail: chaoxi8832@163.com

† Electronic supplementary information (ESI) available. See DOI: https://doi.org/10.1039/d2ra07243b

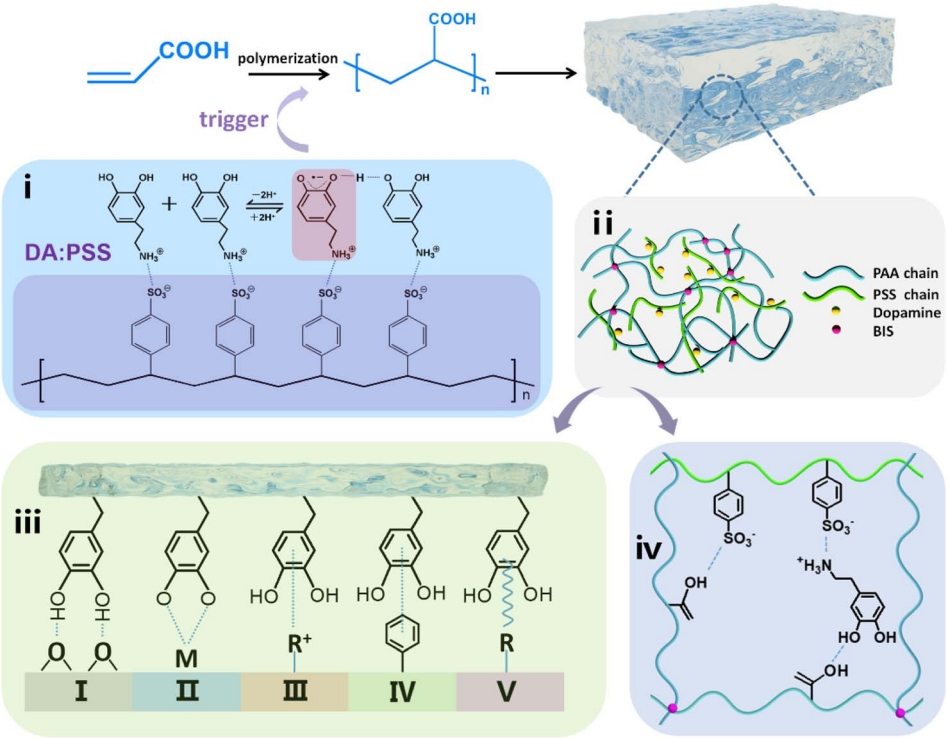

Scheme 1 Schematic of DA:PSS-initiated polymerization-triggered synthesis of PAA adhesive hydrogel. (i) The sulfonate in PSS interacts with the amino group on DA. (ii) Schematic diagram of the internal structure of the hydrogel. (iii) Interactions between the hydrogel and various substrates: (I) hydrogen bond. (II) Coordination bond. (III) Cation–π interaction. (IV) π–π interaction. (V) Covalent linking. (iv) Schematic diagram of interactions of DA, PAA and PSS.

polymerization; during the process, while more semiquinone radicals are found to be produced, dopaquinone is not detected.[24] Furthermore, PSS could be used as the hard segment to interact with flexible macromolecules such as poly(acrylic acid) (PAA) to form interpenetrating polymer network.[25,26] On the other hand, PAA-based hydrogel is an ionic hydrogel which is widely used as flexible wearable sensors due to its excellent ionic conductivity.[25–29]

Here, we prepared an adhesive hydrogel using acrylic acid (AA) as the monomer and *N*,*N*′-methylenebis(acrylamide) (BIS) as the chemical crosslinking agent, initiated by the semiquinone radicals in DA:PSS, where DA:PSS can interact with PAA through hydrogen bond, PSS and PAA could also form interpenetrating network (Scheme 1). The prepared DA:PSS/PAA hydrogel was found to exhibit long-lasting adhesion due to the acidic environment endowed by PAA and the interaction between the amino group of DA and sulfonate of PSS, which prevent the oxidation of DA to dopaquinone. Furthermore, the DA:PSS/PAA hydrogel could be used as flexible wearable sensors.

2. Experimental section

2.1 Materials

Dopamine hydrochloride (DA·HCl, ≥98.0%) was received from Beijing J&K Technology Co., Ltd. Poly(sodium 4-styrenesulfonate) (PSS, $M_w \approx 80\,000$) was purchased from Shanghai McLean Biochemical Technology Co., Ltd. Acrylic acid (AA, ≥99.0%) was purchased from Chengdu Shuobo Research and Innovation Technology Co., Ltd. *N*,*N*′-Methylenebis(acrylamide) (BIS, ≥98.5%) and Tris (hydroxymethyl)aminomethane (Tris, ≥99.5%) were purchased from Chengdu Kelon Chemical Co., Ltd. Ammonium persulfate (APS, ≥98.0%) and acrylamide (AM, ≥98.0%) were purchased from Chengdu Jinshan Chemical Reagent Co., Ltd. *N*-Isopropylacrylamide (NIPAM, ≥98.0%) was purchased from TCI (Shanghai) Development Co., Ltd. Deionized water (18.25 MΩ, 25 °C) generated from a Milli-Q plus purification system (Millipore) was used in all the experiments. Unless otherwise noted, all materials were obtained from commercial supplies and used as received without further purification.

2.2 Preparation of DA:PSS

DA:PSS was prepared according to the previous report.[24] Typically, 1.818 mL PSS was dissolved in the Tris–HCl buffer solution (pH ≈ 8.5) and the mixed solution was stirred for 5 min. Subsequently, 1 g DA·HCl was added and stirred for 12 h at room temperature and pressure, DA:PSS was obtained.

2.3 Preparation of DA:PSS/PAA hydrogel and PSS/PAA hydrogel

Firstly, 1 mL DA:PSS and 1 mL AA (14.587 mmol) were mixed and stirred for 10 min under N_2. Subsequently, 1 mL BIS (0.013

mmol) and 2 mL deionized water were added to the above solution and stirred for another 10 min under N_2. Finally, the above solution was injected into the mold and DA:PSS/PAA hydrogel was formed in an oxygen-free environment after 1 h. DA:PSS/PAA hydrogels with different raw material ratios were prepared by the same method.

As a control, pristine PSS/PAA hydrogel was synthesized by traditional free radical polymerization of AA in the presence of APS (1 mL, 0.0876 mmol) at 60 °C for 4 h. The dosages of AA, BIS, PSS, and Tris in PSS/PAA hydrogel were all consistent with those in DA:PSS/PAA hydrogel, and the total volume was kept at 5 mL.

2.4 Preparation of DA:PSS/PAM hydrogel and DA:PSS/PNIPAM hydrogel

To extend the universality of our strategy, other acrylate monomers were employed to carry out similar experiments. Firstly, 1 mL DA:PSS and 2 mL pH = 2 acrylate monomers (AM or NIPAM) were mixed together and stirred for 10 min under N_2. Subsequently, 1 mL BIS (0.013 mmol) and 1 mL deionized water were added and then stirred for 10 min under N_2. Finally, the above solution was injected into the mold and DA:PSS/PAM hydrogel or DA:PSS/PNIPAM hydrogel was formed in an oxygen-free environment after 2 h. NIPAM was recrystallized before being used.

2.5 Gelation time

The gelation time of the hydrogel was characterized by the vial inverting method. Briefly, the reaction mixture solution (5 mL) was poured into a vial and then incubated in an oxygen-free environment. When the bottle was inverted vertically, no visible flow within 60 s was considered as a standard for gel formation. All experiments were performed in triplicate.

2.6 Mechanical tests

The mechanical properties of hydrogels were measured by a universal tensile machine (QX-W200, Shanghai Qixiang Testing Instrument Co., Ltd.) equipped with a microcomputer at room temperature. The hydrogels used for the test were cylindrical with a diameter of 4.5 mm and a length of 30 mm. The stretching speed was constant at 100 mm min^{-1}. All experiments were repeated 3 times and the mean value was reported. The tensile strength is defined as:

$$\sigma = F/A_0 \quad (1)$$

where σ is the tensile strength (Pa), F is the tensile load (N), A_0 is the initial cross-sectional area of the hydrogels (m^2).

2.7 Adhesion tests

The adhesion behaviors of DA:PSS/PAA hydrogel were characterized by the lap-shear test. Two pieces of substrates were stick together by the hydrogel with the bonding area of 10 × 10 mm^2, pressed by pressure of 1 kPa for 10 s in air at ambient temperature without any additional treatment, and then the external pressure was removed immediately. The maximum stress during shear adhesive tests was recorded as the adhesive strength, calculated by the maximum force divided by the initial bonding area. The adhesion-peel cycles experiments were completed within 15 minutes. For testing the adhesion properties of the DA:PSS/PAA hydrogel after 21 days, the hydrogel was placed in an airtight container with a small amount of moisture to maintain a humidity at 76% RH for 21 days, and then the adhesion properties were characterized.

2.8 Anti-drying tests

The hydrogel samples were attached to the skin of the subject's arm, which were exposed at room temperature and the weight changes were recorded after 5 hours (room temperature: 18 °C, body temperature: 36.5–36.8 °C, air humidity: 60% RH). The weight loss ratio (WLR) was calculated according to the following formula:

$$\mathrm{WLR} = (W_0 - W)/W_0 \times 100\% \quad (2)$$

where, WLR is the weight loss ratio, W_0 is the initial mass of the hydrogel, and W is the mass of the hydrogel after attached to the skin for 5 hours.

2.9 Electrical properties tests

The resistance of hydrogel was measured by the compact LCR digital bridge of TH283X. The sensitivity of a strain sensor was usually evaluated in terms of the gauge factor (GF), which was estimated as follows:

$$\mathrm{GF} = (\Delta R/R_0)/\varepsilon \quad (3)$$

where ΔR is the measured resistance (R) minus the initial resistance (R_0), and ε is the applied strain. In human motion experiments, the hydrogel attached to the sensor adhered directly to the skin to detect the change of resistance under different states of motion.

3. Results and discussion

3.1 Analysis of the chemical structure of DA:PSS

The complex of DA and PSS (DA:PSS) was synthesized by directly adding solid DA·HCl into an aqueous solution of PSS, according to the method described in the literature.[24] The structure of DA:PSS is obtained from the ^{1}H-NMR and ^{13}C-NMR spectra of DA:PSS and DA·HCl, respectively, as shown in Fig. 1. The peaks at around 6.5 ppm belonged to the aromatic protons of DA in DA:PSS. Moreover, there were two sharp peaks at 9.0 ppm, which may be ascribed to the phenolic hydroxyl protons of DA in DA:PSS (Fig. 1a). The ^{1}H-NMR spectra of DA·HCl and DA:PSS overlapped almost completely. The signal peaks in the ^{1}H-NMR spectra of DA:PSS were very clear and were completely different from those in the ^{1}H-NMR spectra of PDA.[24] The ^{13}C-NMR spectra of DA:PSS matched well with that of the DA monomer (Fig. 1b). The ^{1}H-NMR and ^{13}C-NMR spectra showed the structure of DA:PSS similar to that shown in the literature,[24] indicating that no dopaminequinone was generated. These results show that we have successfully synthesized DA:PSS.

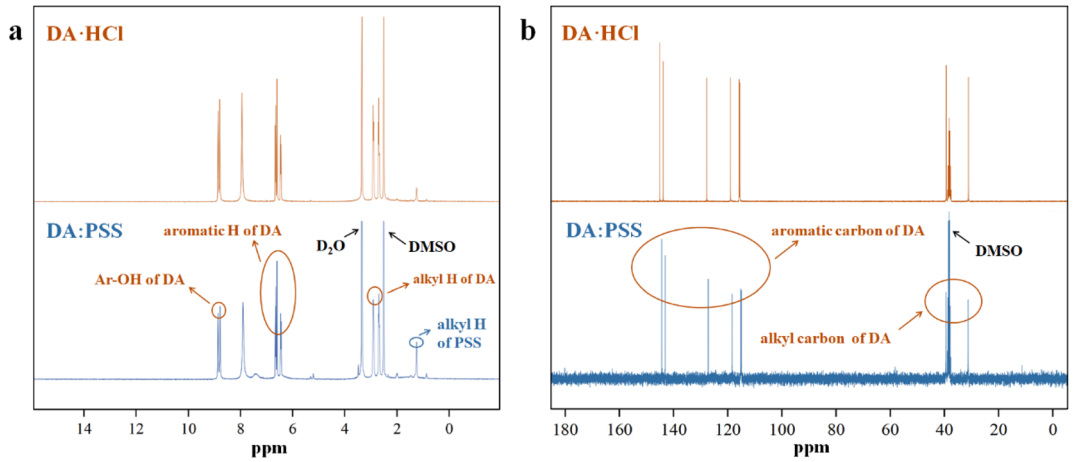

Fig. 1 (a) ^{1}H-NMR and (b) ^{13}C-NMR spectra of DA·HCl and DA:PSS.

Electron spin resonance (ESR) was conducted to detect the characteristics of radicals in DA:PSS (Fig. S1†). A single-line ESR of DA:PSS with accurate *g*-factor of 2.0050 (the experimental data amounted to 2.0010) at room temperature was detected, indicating the formation of semiquinone radicals.[24,30] Thus, the semiquinone radicals in DA:PSS could be used to trigger free radical polymerization.

3.2 Mechanical properties of DA:PSS/PAA hydrogel

According to previous reports, PAA and PSS chains could form interpenetrating networks in which PAA interacts with DA and PSS *via* hydrogen bonding.[25,26,31,32] In this work, gelation time experiments were used to explore the appropriate ratio of spontaneous formation of hydrogels by DA:PSS and AA without adding initiators (Fig. S2 and S3†). It could be observed that the gelation time decreased with the increase in the dosage of DA:PSS. The weight ratio of DA:PSS to AA was chosen as 1 : 1 for the subsequent experiments. However, the strength of these hydrogels was so low that limited their application. To obtain hydrogels with good mechanical properties, crosslinking agent BIS was induced into the reaction system, which could adjust the crosslinking density of the hydrogels. Composite hydrogels with different mechanical properties were obtained by changing the content of BIS. Fig. 2a shows the stress–strain curves of the DA:PSS/PAA hydrogel with different BIS contents. It could be seen that, as the BIS content increased from 0.001 to 0.016 g, the stress of the composite hydrogels also increased from 28.7 kPa to ~50.8 kPa and the elongation at break reduced from 1879% to ~206%. Due to the addition of BIS, the hydrogel forms multi-crosslinking points that increase the rigidity of the hydrogel and reduce the toughness.[33] The DA:PSS/PAA hydrogel exhibits proper mechanical strength (44.9 kPa) and good stretchability (1249%) at the BIS content of 0.002 g mL^{-1}. The tensile modulus (100–200% strain) and toughness of DA:PSS/PAA hydrogel at the BIS content of 0.002 g mL^{-1} are 6.61 kPa, 30.479 kJ m^{-2}, respectively. Considering at strain and tensile strength, 0.002 g mL^{-1} BIS was used for subsequent experiments.

Interestingly, this DA:PSS-initiated strategy applies equally to other acrylate monomers such as AM and NIPAM as well.

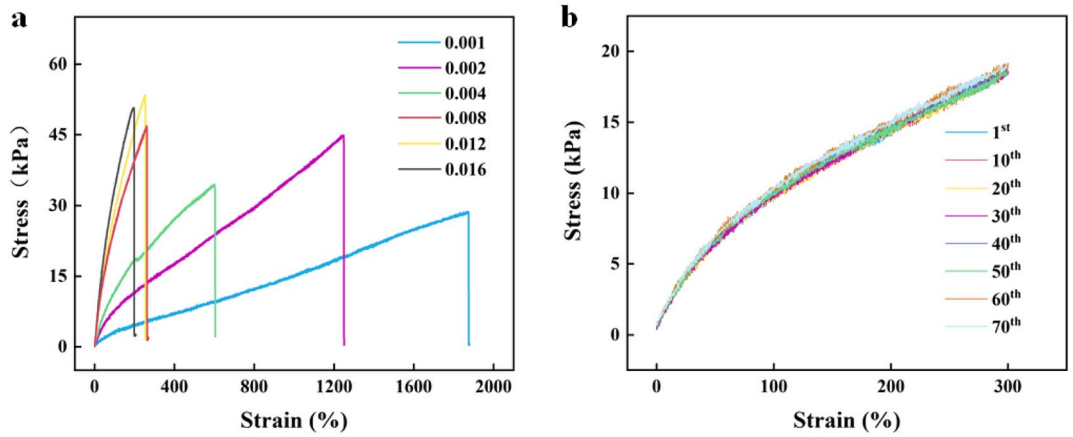

Fig. 2 Mechanical properties of the DA:PSS/PAA hydrogel. (a) Stress–strain curves of the DA:PSS/PAA hydrogel with different BIS contents. (b) Elasticity of the DA:PSS/PAA hydrogel under 70 successive loading–unloading cycles.

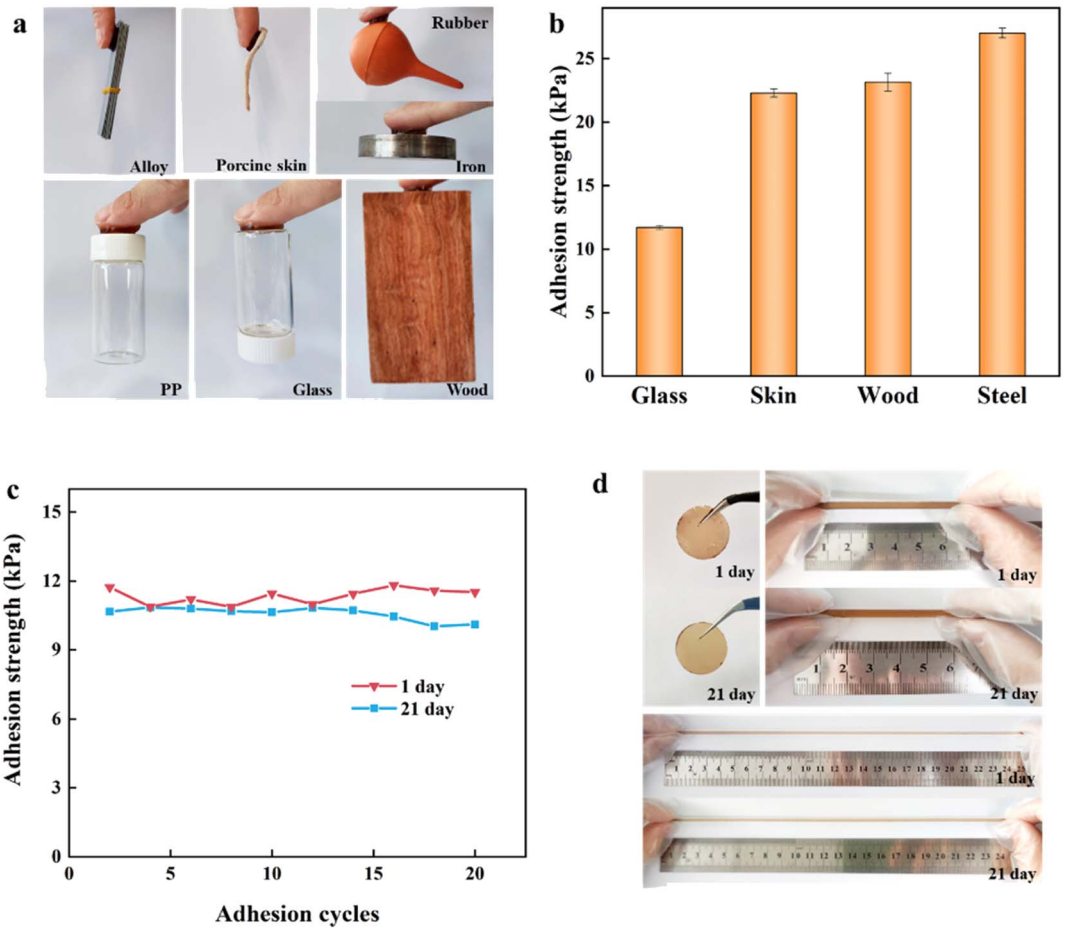

Fig. 3 Adhesion ability of the DA:PSS/PAA hydrogel. (a) DA:PSS/PAA hydrogel showed good adhesion to various substrates: alloys, porcine skin, rubbers, iron, PP, glass, and wood. (b) The adhesion strength of the DA:PSS/PAA hydrogel on different substrates. (c) The adhesion strength of the DA:PSS/PAA hydrogel under 20 adhesion-peel cycles (d) Photographs of the appearance and simple stretching of the DA:PSS/PAA hydrogel after 21 days.

However, only in acidic solutions could AM and NIPAM form hydrogels initiated by semiquinones present in DA:PSS (Fig. S4†). From these observations, it may be preliminarily concluded that pH affects the activity of semiquinones in DA:PSS as the initiators for radical polymerization. The reasons for this will be studied in future works.

Stability is crucial for the practical application of hydrogels. Therefore, we characterized the fatigue properties of the DA:PSS/PAA hydrogel (Fig. 2b). As shown in Fig. 2b, DA:PSS/PAA hydrogel had no obvious hysteresis in their stress–strain curves even after 70 cycles of continuous tension recovery test, with a tensile deformation of 300%, indicating that the DA:PSS/PAA hydrogel has good fatigue resistance. These results indicated that DA:PSS/PAA hydrogel had good mechanical properties. Fig. S5† shows a comparison of the properties of the PSS/PAA hydrogel (using APS as the initiator) and of the DA:PSS/PAA hydrogel. It may be seen that the elongation of the DA:PSS/PAA hydrogel (1249%) is far greater than that of the PSS/PAA hydrogel (618%), which is due to the multiple hydrogen bonds and ionic interaction induced by DA in the DA:PSS/PAA network.[12,34]

3.3 Adhesion properties of DA:PSS/PAA hydrogel

As shown in Fig. 3a, DA:PSS/PAA hydrogel could adhere to the surface of PP, alloys, porcine skin, rubbers, iron, glass, and wood. The adhesion strength of DA:PSS/PAA hydrogel on different substrates including glass, porcine skin, wood, and steel were found to be 11.7, 22.3, 23.2, and 27.0 kPa, respectively (Fig. 3b), which is very comparable with some catechol-based hydrogels.[12,35] In addition, the adhesion strength of the DA:PSS/PAA hydrogel (newly prepared and after 21 days storage) on glass remained almost unchanged even after 20 peel-adhesion cycles, which indicated that the DA:PSS/PAA hydrogel has long-lasting and repeatable good adhesion (Fig. 3c). The photographs of the DA:PSS/PAA hydrogel showed that the colour of the hydrogel changed only slightly after 21 days (Fig. 3d), indicating that the catechol hardly oxidized in the hydrogel due to the acidic environment and the interaction between the amino group of DA and sulfonate of PSS.[24]

Furthermore, two DA:PSS/PAA hydrogels was put on the arm crossing the wrist for 5 hours to investigate the effect of the real body and around environment on this hydrogel (Fig. S6†). In comparison, one of the DA:PSS/PAA hydrogels was coated with

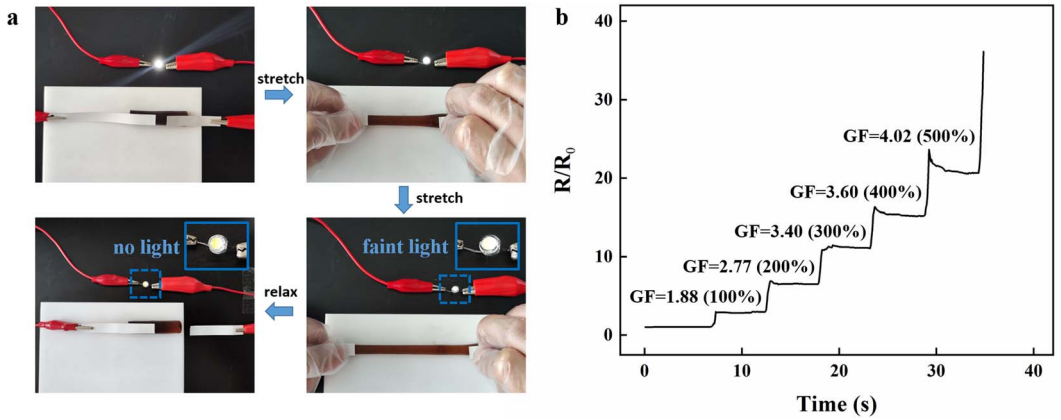

Fig. 4 Strain-responsive conductivity properties of the DA:PSS/PAA hydrogel. (a) Change in the LED light with the elongation of the hydrogel. (b) Change in the resistance and GF values of the DA:PSS/PAA hydrogel with increasing strain.

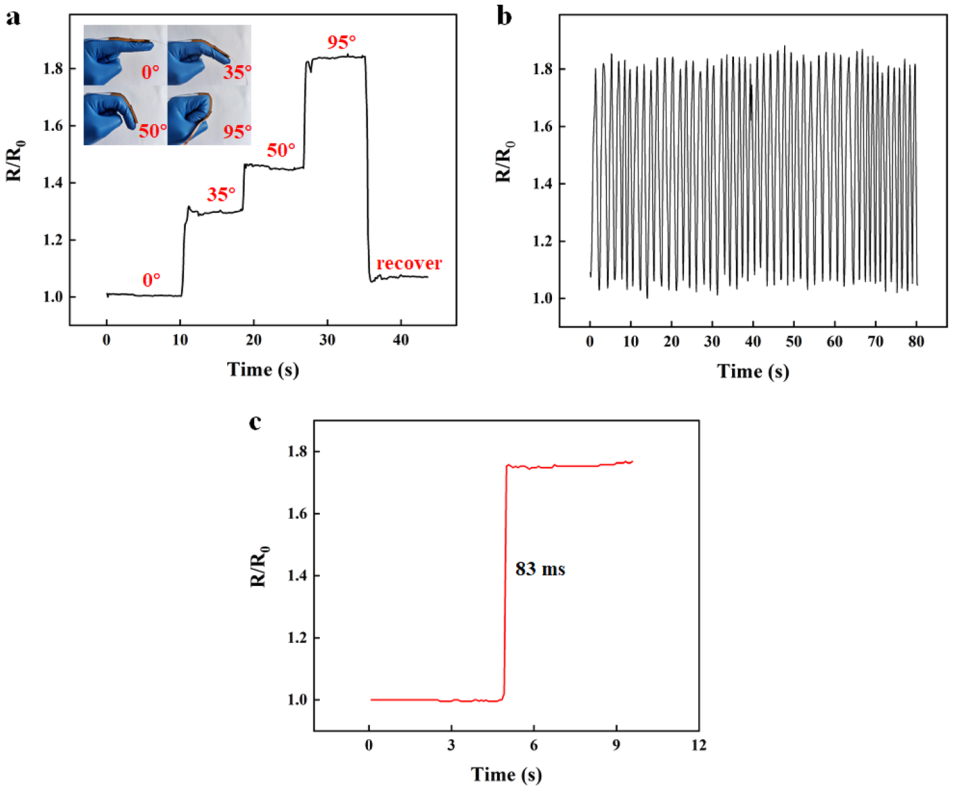

Fig. 5 Electromechanical properties of the DA:PSS/PAA hydrogel. (a) Relative resistance variations of the hydrogel strain sensors adhered onto the finger bending upon different angles (0°, 35°, 50°, and 95°). (b) Stability tests of the hydrogel sensors by repeatedly applying for multiple cycles. (c) The response times were up to 83 ms.

glycerine after adhered to the arm. It was observed that both hydrogels turned thinner, indicating the losing of water happened for both hydrogels due to the body temperature. But it was apparent that the hydrogel coated with glycerine kept more water than that of the bare hydrogel. And the calculation of weight loss supported the observation (65.03% for the bare hydrogel and 54.37% for the hydrogel coated with glycerin). The weight loss changed the mechanical properties as shown in Fig. S7.† To make the prepared hydrogel meet the practical application, the improvement of moisture retention was necessary, and the related work will be carried out later.

The adhesion of the DA:PSS/PAA hydrogel may be attributed to the synergistic effect of the carboxyl groups of PAA, sulfonate groups of PSS, and the catechol groups of DA through covalent and noncovalent bonding, as shown in Scheme 1. The existence of large amounts of hydrogen bonds and electrostatic interactions in this system is of great importance to the adhesive properties. In addition to the interaction between the hydrogen

bonds and electrostatic interactions, other physical interactions that are formed between the gel and the substrate, such as π–π stacking, cation–π interaction, and metal coordination,[12,16,19,36–38] are also expected also endow the hydrogel materials with adhesiveness.

3.4 Strain-responsive conductivity properties of DA:PSS/PAA hydrogel

The DA:PSS/PAA hydrogel demonstrated good electrical conductivity due to the presence of Na^+ of PSS in the network, serving as a conductive medium. The circuit was formed by connecting the hydrogel with copper wires, an LED bulb, and a power supply. Upon stretching, the brightness of the LED bulb darkened and the brightness recovered when the strain disappeared. It may be noted that the brightness of the LED bulb changed almost simultaneously with stretching, revealing the fast response of the hydrogel to strain. Fig. 4a shows the change in resistance of the DA:PSS/PAA hydrogel when it is stretched to different lengths. It can be seen in Fig. 4b that, as the hydrogel is stretched continuously, its resistance increases immediately with hardly any hysteresis. We further use the gauge factor (GF, $(\Delta R/R_0)/\varepsilon$) to evaluate the strain sensitivity. Within the strain increases to 500%, the GF was found to be 4.02. Therefore, it may be concluded that the DA:PSS/PAA hydrogel has the potential to be used as a skin sensors.

3.5 Flexible wearable sensors based on DA:PSS/PAA hydrogel

Given their excellent flexibility, strain sensitivity, and adhesive ability, DA:PSS/PAA hydrogel was able to be applied as a wearable strain sensor to detect the motions of finger. To monitor finger motion, we attached the hydrogel sensor to the finger and recorded the real-time resistance–time curve in finger flexion by the electrochemical workstation. The relative resistance change with the finger flexion is shown in Fig. 5a. By bending the fingers (0°, 35°, 50°, and 95°), the change in the hydrogel resistance at different angles was detected. When the finger bending increased from 35° to 50° to 95°, the resistance was also found to increase gradually. When the finger was bent back to 0°, the original resistance was recovered. The relative resistance of the hydrogel increased as the flexion angle of the finger increased. As the hydrogel was attached to the finger, it readily stretched upon finger flexion, leading to an increase in the resistance. With a stepwise increase in the flexion angle of the finger, the relative resistance also showed a corresponding stepwise increase. The relative resistance changes under finger motion also showed a fast and repeatable response, with response times up to 83 ms (Fig. 5b and c). The finger motion monitoring results proved that DA:PSS/PAA hydrogel could be used as flexible wearable sensors to detect human activities due to their high sensitivity.

4. Conclusions

In summary, we report a polymerization strategy to fabricate catechol-functionalized hydrogel triggered by semiquinone radicals in DA:PSS. The DA:PSS/PAA hydrogel exhibits good stretchability (1249%) due to the existence of the interpenetrating network of PAA and PSS, and the multiple hydrogen bonds induced by DA. In contrast, profiting from the abundant catechol, carboxyl, and sulfonate groups, the conductive hydrogel presented good adhesion with various substrates (*e.g.*, PP, alloys, porcine skin, rubbers, iron, glass, and wood). Additionally, the DA:PSS/PAA hydrogel has long-lasting adhesiveness, which may be attributed to the resistance of DA to oxidation due to the acidic environment and the interaction of the amino group of DA and sulfonate group of PSS. The DA:PSS/PAA hydrogel also exhibits strain-responsive conductivities. Attributed to these advantages, the conductive DA:PSS/PAA hydrogel could be applied as skin-like sensors to monitor human movements. To meet the long-term application, it is necessary to improve the moisture retention of the DA:PSS/PAA hydrogel. We are continuing our research to find out how pH affects the activity of semiquinones in DA:PSS, and develop proper methods to improve the moisture retention of the prepared hydrogels. We believe that our work may provide new insights into the development of adhesive hydrogels based on DA and PDA materials.

Conflicts of interest

The authors declare that they have no known competing financial interests or personal relationships that could have appeared to influence the work reported in this paper.

Acknowledgements

This work was supported by the National Natural Science Foundation of China (51273220), and Innovative Research Projects for Graduate Students, Southwest Minzu University (ZD2022695). We thank LetPub (**https://www.letpub.com/**) for its linguistic assistance during the preparation of this manuscript.

References

1 Z. Huang, Y. Xu, Y. Cheng, M. Xue, M. Deng, N. Jaffrezic-Renault and Z. Guo, *Sens. Diagn.*, 2022, **1**, 686–708.
2 T. Zhang, L. Meng, Y. Hu, Z. Ouyang, W. Li, B. Xie, F. Zhu, J. Wan and Q. Wu, *RSC Adv.*, 2022, **12**, 23637–23643.
3 C. Wang, T. Yokota and T. Someya, *Chem. Rev.*, 2021, **121**, 2109–2146.
4 Y. Liu, J. Zheng, X. Zhang, Y. Du, G. Yu, K. Li, Y. Jia and Y. Zhang, *RSC Adv.*, 2021, **11**, 14665–14677.
5 H. Zhao, S. Hao, Q. Fu, X. Zhang, L. Meng, F. Xu and J. Yang, *Chem. Mater.*, 2022, **34**, 5258–5272.
6 H. Zhu, J. Xu, X. Sun, Q. Guo, Q. Guo, M. Jiang, K. Wu, R. Cai and K. Qian, *J. Mater. Chem. A*, 2022, **10**, 23366–23374.
7 X. Zhang, J. Chen, J. He, Y. Bai and H. Zeng, *J. Colloid Interface Sci.*, 2021, **585**, 420–432.
8 M. Liao, P. Wan, J. Wen, M. Gong, X. Wu, Y. Wang, R. Shi and L. Zhang, *Adv. Funct. Mater.*, 2017, **27**, 1703852.

9 L. Han, X. Lu, K. Liu, K. Wang, L. Fang, L. T. Weng, H. Zhang, Y. Tang, F. Ren, C. Zhao, G. Sun, R. Liang and Z. Li, *ACS Nano*, 2017, **11**, 2561–2574.
10 X. Jing, H. Y. Mi, Y. J. Lin, E. Enriquez, X. F. Peng and L. S. Turng, *ACS Appl. Mater. Interfaces*, 2018, **10**, 20897–20909.
11 J. Xu, G. Wang, Y. Wu, X. Ren and G. Gao, *ACS Appl. Mater. Interfaces*, 2019, **11**, 25613–25623.
12 C. Zhang, Y. Zhou, H. Han, H. Zheng, W. Xu and Z. Wang, *ACS Nano*, 2021, **15**, 1785–1794.
13 L. Han, K. Liu, M. Wang, K. Wang, L. Fang, H. Chen, J. Zhou and X. Lu, *Adv. Funct. Mater.*, 2018, **28**, 1704195.
14 B. J. Kim, D. X. Oh, S. Kim, J. H. Seo, D. S. Hwang, A. Masic, D. K. Han and H. J. Cha, *Biomacromolecules*, 2014, **15**, 1579–1585.
15 H. Lee, S. Dellatore, W. Miller and P. Messersmith, *Science*, 2007, **318**, 426–430.
16 C. Zhao, F. Zuo, Z. Liao, Z. Qin, S. Du and Z. Zhao, *Macromol. Rapid Commun.*, 2015, **36**, 909–915.
17 Y. Liu, K. Ai and L. Lu, *Chem. Rev.*, 2014, **114**, 5057–5115.
18 H. Liu, X. Qu, H. Tan, J. Song, M. Lei, E. Kim, G. F. Payne and C. Liu, *Acta Biomater.*, 2019, **88**, 181–196.
19 W. Zhang, Z. Liao, X. Meng, A. Ai Niwaer, H. Wang, X. Li, D. Liu and F. Zuo, *Appl. Surf. Sci.*, 2020, **527**, 146821.
20 M. D. Nothling, C. G. Bailey, L. L. Fillbrook, G. Wang, Y. Gao, D. R. McCamey, M. Monfared, S. Wong, J. E. Beves and M. H. Stenzel, *J. Am. Chem. Soc.*, 2022, **144**, 6992–7000.
21 J. V. Paulin, A. Batagin-Neto, P. Meredith, C. F. O. Graeff and A. B. Mostert, *J. Phys. Chem. B*, 2020, **124**, 10365–10373.
22 Z. Liao, W. Zhang, Z. Qiao, J. Luo, A. E. Ai Niwaer, X. Meng, H. Wang, X. Li, F. Zuo and Z. Zhao, *J. Colloid Interface Sci.*, 2020, **562**, 81–90.
23 C. Zhang, M. Q. Ma, T. T. Chen, H. Zhang, D. F. Hu, B. H. Wu, J. Ji and Z. K. Xu, *ACS Appl. Mater. Interfaces*, 2017, **9**, 34356–34366.
24 W. Liang, L. Xu, S. Sun, L. Lan, X. Qiu, R. Chen and Y. Li, *ACS Sustainable Chem. Eng.*, 2016, **5**, 460–468.
25 Q. Gao, C. Li, M. Wang, J. Zhu, D. Munna, P. Wang, C. Zhu, J. Gao and C. Gao, *J. Mater. Chem. C*, 2022, **10**, 6271–6280.
26 L. Dong, M. Wang, J. Wu, C. Zhu, J. Shi and H. Morikawa, *ACS Appl. Mater. Interfaces*, 2022, **14**, 9126–9137.
27 Y. Jiao, Y. Lu, K. Lu, Y. Yue, X. Xu, H. Xiao, J. Li and J. Han, *J. Colloid Interface Sci.*, 2021, **597**, 171–181.
28 Y. Zhang, X. Tian, Q. Zhang, H. Xie, B. Wang and Y. Feng, *J. Bioresour. Bioprod.*, 2022, **7**, 116–127.
29 Y. Jiao, K. Lu, Y. Lu, Y. Yue, X. Xu, H. Xiao, J. Li and J. Han, *Cellulose*, 2021, **28**, 4295–4311.
30 S. Du, Y. Luo, Z. Liao, W. Zhang, X. Li, T. Liang, F. Zuo and K. Ding, *J. Colloid Interface Sci.*, 2018, **523**, 27–34.
31 S. Cao, X. Tong, K. Dai and Q. Xu, *J. Mater. Chem. A*, 2019, **7**, 8204–8209.
32 Y. Wang, Y. Shen, Y. Zhang, B. Yue and C. Wu, *J. Macromol. Sci., Part B: Phys.*, 2006, **45**, 563–571.
33 P. Li, W. She, Y. Luo, D. He, J. Chen, N. Ning, Y. Yu, S. de Beer and S. Zhang, *J. Mater. Chem. B*, 2021, **9**, 159–169.
34 Z. Jia, Y. Zeng, P. Tang, D. Gan, W. Xing, Y. Hou, K. Wang, C. Xie and X. Lu, *Chem. Mater.*, 2019, **31**, 5625–5632.
35 C. Shao, M. Wang, L. Meng, H. Chang, B. Wang, F. Xu, J. Yang and P. Wan, *Chem. Mater.*, 2018, **30**, 3110–3121.
36 X. Fan, Y. Fang, W. Zhou, L. Yan, Y. Xu, H. Zhu and H. Liu, *Mater. Horiz.*, 2021, **8**, 997–1007.
37 X. Su, Y. Luo, Z. Tian, Z. Yuan, Y. Han, R. Dong, L. Xu, Y. Feng, X. Liu and J. Huang, *Mater. Horiz.*, 2020, **7**, 2651–2661.
38 D. Gan, Z. Huang, X. Wang, L. Jiang, C. Wang, M. Zhu, F. Ren, L. Fang, K. Wang and C. Xie, *Adv. Funct. Mater.*, 2020, **30**, 1907678.